

1 SUPPORTING INFORMATION A

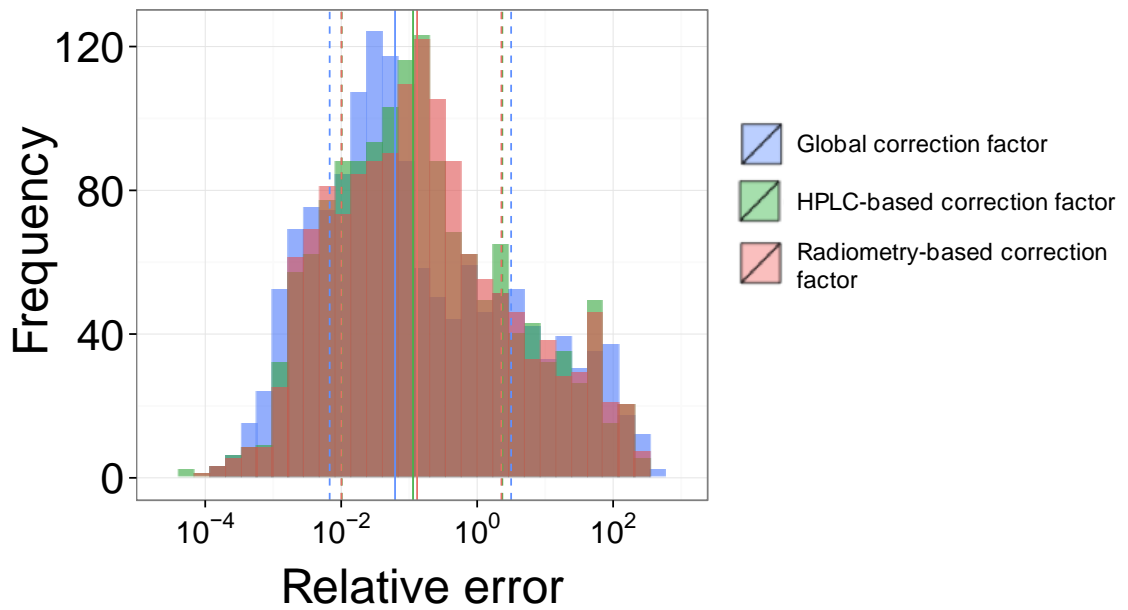
2 The BGC-Argo database used in this paper relies on *in vivo* chlorophyll fluorescence
3 measurements as a proxy for the chlorophyll *a* concentration (Chl*a*). The calibration of the
4 chlorophyll fluorescence signal into Chl*a* is challenging because the fluorescence-to-
5 chlorophyll ratio shows large variability (*Falkowski and Kiefer, 1985*) depending on several
6 factors, including sensor characteristics as well as environmental conditions and biology (e.g.
7 phytoplankton photophysiology, taxonomic composition) (*Cleveland et al., 1989; Geider et*
8 *al., 1997; Dubinsky and Stambler, 2009*). Despite those limitations, *in vivo* fluorescence
9 represents an easy, cost-effective way for measuring Chl*a*. It can be measured over broad
10 ranges of space and temporal scales from small fluorometers installed on a variety of
11 platforms such as BGC-Argo floats.

12 The advent and increasing use of BGC-Argo floats led the community to develop
13 standard procedures, recognized at an international level, to be applied for the calibration and
14 qualification of the bio-optical proxies measured by the floats (*Schmechtig et al., 2014, 2016*).
15 Recently, however, *Roesler et al. (2017)* have reported a systematic overestimation in the
16 calibrated Chl*a* values derived from WET Labs ECO-series sensors (i.e. identical to those
17 installed on BGC-Argo floats), and recommended a correction factor of 2 to be applied
18 globally at the user level. This recommendation was based on the analysis of a match-up
19 database of HPLC Chl*a* determinations and calibrated *in situ* fluorescence observations from
20 WET Labs ECO fluorometers. Their results were further supported by comparisons of
21 calibrated fluorescence observations with Chl*a* values derived from other techniques, e.g.
22 radiometric measurements (*Xing et al., 2011*), light absorption line height (*Roesler and*
23 *Barnard, 2013*), experiments on algal cultures.

24 The study of *Roesler et al. (2017)*, deals with two distinct issues that have to be

25 independently considered. On the one hand, the global correction factor of 2 addresses an
26 instrumental bias and allows a better correction of the WET Labs ECO-series fluorometers.
27 On the other hand, this correction factor may vary regionally as a result of natural variations
28 in the fluorescence-to-chlorophyll ratio. *Roesler et al. (2017)* proposed regional correction
29 factors from the analysis of the database of paired HPLC-determined Chla measurements and
30 calibrated *in situ* chlorophyll fluorescence observations. The regional factors were computed
31 for 10 of the *Longhurst (2006)* biogeographic regions where data were available. In addition,
32 for 16 Longhurst's regions where BGC-Argo floats collected radiometric data, the authors
33 computed regional correction factors based on a comparison of the Chla values obtained from
34 the fluorescence observations calibrated using either the standard procedure or the
35 "radiometric" calibration method of *Xing et al. (2011)*. In brief, this method is based on a bio-
36 optical relationship that links the Chla values to the diffuse light attenuation coefficient (K_d)
37 as derived from the downwelling irradiance (E_d) measurements acquired by BGC-Argo floats
38 (*Morel et al., 2007a*).

39 First, we looked at the impact of these different regional correction factors on the
40 distribution of the computed errors in the b_{bp} -to-Chla ratio. We analysed the relative error in
41 the b_{bp} -to-Chla ratio computed following the method described in Section 2.2.3 of the
42 manuscript using the global as well as the regional HPLC- and radiometry-based correction
43 factors (Figure A1). The results suggest similar distribution of the b_{bp} -to-Chla relative errors
44 regardless of the factor applied to correct the Chla values at a statistical significance level of
45 0.01.

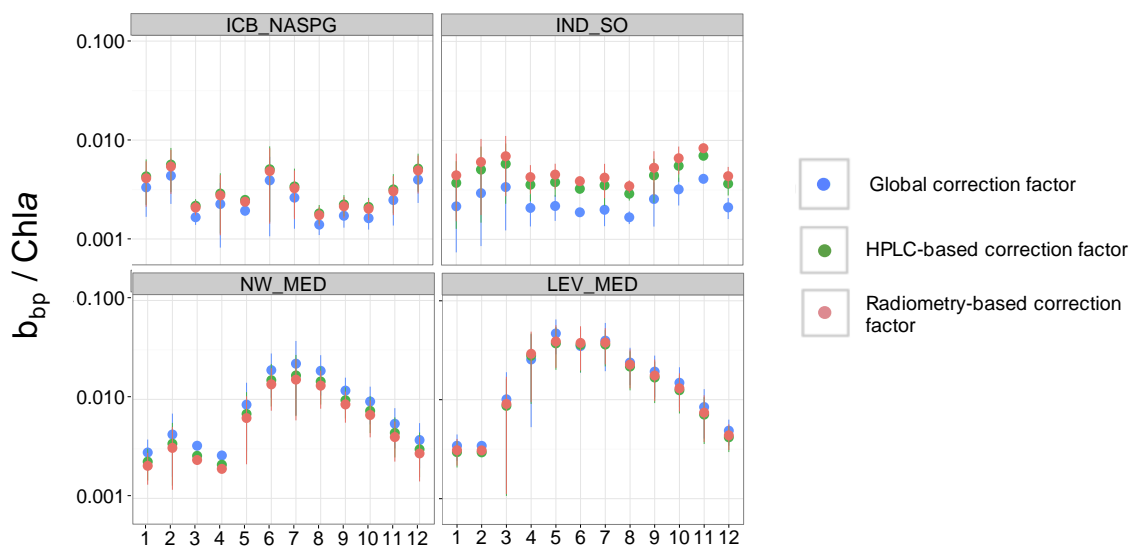


46
 47 **Figure A1:** Histogram of the distribution of the relative error in the b_{bp} -to- $Chla$ ratio for the
 48 $0-Z_{pd}$ layer; the plain lines indicate the median error and dotted lines the 20% and 80%
 49 quantile.

50 It appears that correcting the fluorescence-based $Chla$ values of the database with
 51 regional factors compared to a global factor does not significantly affect the distribution of the
 52 computed errors in the b_{bp} -to- $Chla$ ratio.

53 Second, we performed an analysis of the sensitivity of the b_{bp} -to- $Chla$ relationship to
 54 *Roesler et al. (2017)* regional correction factors. At a regional scale, we tested the influence of
 55 applying the regional HPLC- and radiometry-derived correction factors, compared to the
 56 global factor of 2, on the variability of the b_{bp} -to- $Chla$ ratio. The regional HPLC-based factors
 57 are available for four regions of our database: Icelandic Basin of North Atlantic Subpolar
 58 Gyre (ICB_NASPG), Indian Sector of the Southern Ocean (IND_SO), North-western
 59 Mediterranean Sea (NW_MED) and Levantine Sea (LEV_MED). Those factors were,
 60 respectively, 2.6 ± 0.78 , 3.46 ± 0.35 , 1.62 ± 0.28 and 1.72 ± 0.23 . The radiometry-based factors for
 61 the same regions were, respectively, 2.49 ± 0.31 , 4.13 ± 0.65 , 1.47 ± 0.12 and 1.80 ± 0.11 . In the

62 ICB_NASPG and IND_SO, the Chla values are underestimated when the global factor of 2 is
 63 applied compared to the regional factors (>2). In contrast, the Chla is overestimated in the
 64 NW and the LEV_MED. Figure A2 shows the seasonal variability of the b_{bp} -to-Chla ratio
 65 with the Chla originating from the global correction factor or from the regional HPLC- or
 66 radiometry-based factors. Because the regional factors are constant over a given region, our
 67 regional interpretation of the b_{bp} -to-Chla ratio seasonal variations remains essentially
 68 unchanged (Figure A2).



69

70 **Figure A2:** Monthly climatology of the b_{bp} -to-Chla ratio within the surface layer ($0-Z_{pd}$) for
 71 the four regions where regional HPLC- and radiometry-derived correction factors are
 72 available.

73 At a global scale, we examined the impact on the b_{bp} -to-Chla relationships in the
 74 different layers of the water column, of the application of the global factor of 2 *versus* the
 75 regional radiometry-based factors. This global-scale analysis has been conducted using the
 76 radiometry-based factors that were available for 20 of the 24 regions of our BGC-Argo
 77 database. It could not be performed with the HPLC-based factors, available for only 4 regions
 78 of our database. The results are presented in Figure A3 and Table A1; Figure A3 is similar to
 79 Figure 3 of the manuscript but uses the regional radiometry-based factors instead of the global
 80 factor of 2. The radiometry-derived correction factors do not significantly alter the b_{bp} -to-

81 Chla relationship in the different layers of the water column as suggested by the results of a
82 significance test (mentioned in Table A1). The most noticeable change shown in Figure A3,
83 compared to Figure 3 of the manuscript, is observed for the Southern Ocean. This region of
84 the global ocean has been reported to have an atypical bio-optical status (*Organelli et al.*,
85 2017a), so that the regional radiometry-derived factors may be questionable. The Southern
86 Ocean is also the largest High Nutrient Low Chlorophyll (HNLC) region of the global ocean,
87 with large spatio-temporal variability in iron stress (e.g., *Boyd et al.*, 2000; *Blain et al.*, 2007).
88 The potential impact of iron limitation on the fluorescence-to-chlorophyll ratio (*Behrenfeld et*
89 *al.*, 2006) should be investigated further in the Southern Ocean and in other HLNC regions
90 such as the Subequatorial or North Pacific.

91 For the other regions of our database, the trend and scattering of the data points
92 observed for the different layers of the water column remain similar regardless of the
93 considered global or regional correction factors. The statistical indices R^2 and RMSE are only
94 slightly modified and the slopes and intercepts of the b_{bp} -to-Chla relationships remain almost
95 identical (see Table A1).

96

97

98

99

100

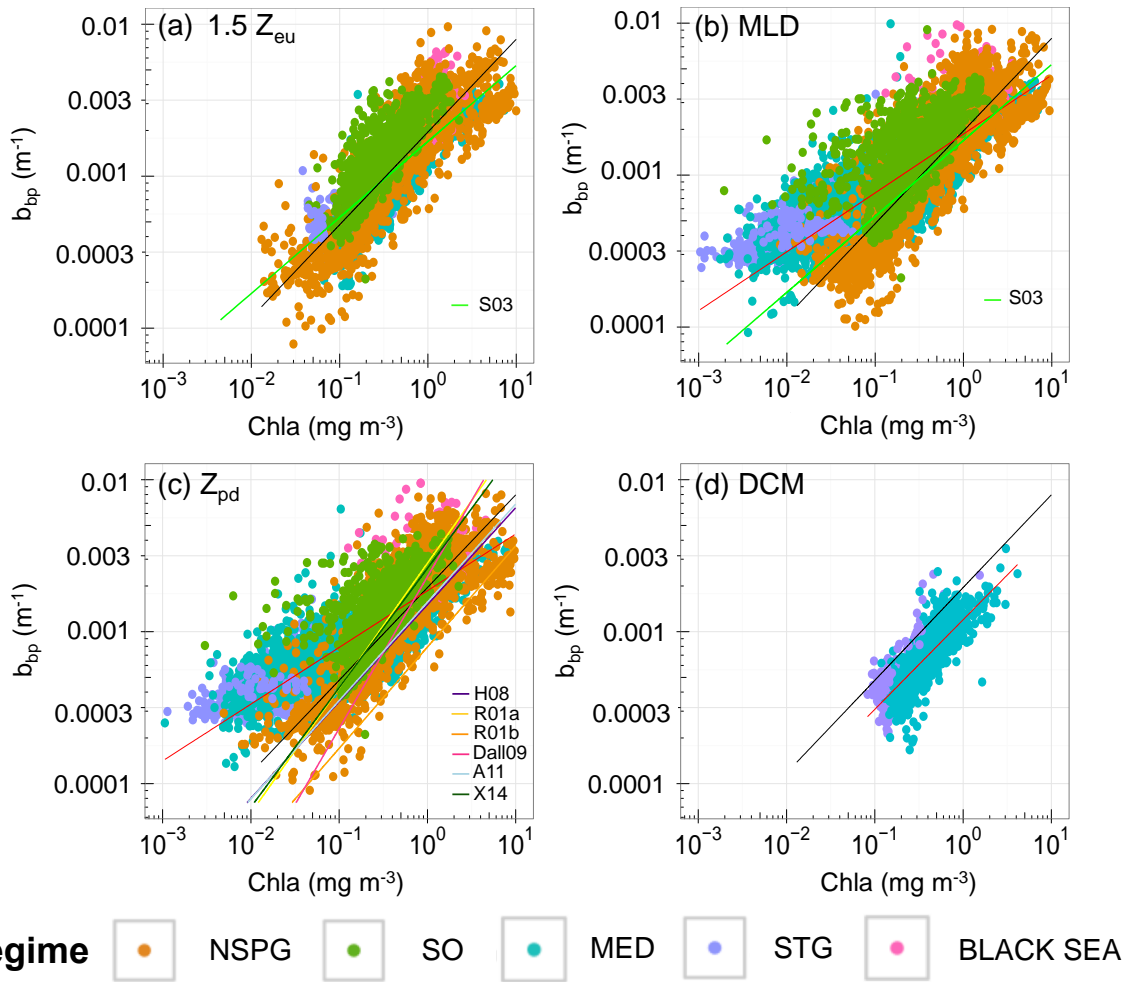
101

102

103

104

105



106

107 **Figure A3:** Log-log scatterplot of the particulate backscattering coefficient at 700 nm (b_{bp}) as
108 a function of the chlorophyll a concentration (Chla) corrected using the regional radiometry-
109 derived factors of Roesler et al. (2017) within (a) the productive layer comprised between the
110 surface and $1.5 Z_{eu}$; (b) the mixed layer; (c) the surface ($0-Z_{pd}$) layer and (d) the DCM layer.
111 The color code indicates the regime where the BGC-Argo data were collected. For each plot,
112 the black line represents the relationship calculated over the productive layer ($0-1.5 Z_{eu}$)
113 while the red line represents the regression model calculated over the considered layer.

Table A1. Comparison of the coefficient of determination R^2 , Root Mean Squared Error (RMSE), intercept and slope associated to the b_{bp} -to-Chla relationships with the Chla values resulting from the application of either the global correction factor of 2 or the regional radiometry-derived factors of *Roesler et al.* [2017].

The relationships are not statistically different at a significance level of 0.05 (Wilcoxon test).

Water column layer	Statistical index	Relationship obtained with the global factor of 2	Relationship obtained with the regional radiometry-based factors
0- Z_{pd}	Intercept	0.00174	0.00186
	Slope	0.36	0.373
	RMSE	0.000942	0.000921
	R^2	0.6311	0.6485
0- MLD	Intercept	0.00171	0.00186
	Slope	0.373	0.387
	RMSE	0.000932	0.000969
	R^2	0.6167	0.6339
DCM	Intercept	0.00147	0.00119
	Slope	0.753	0.5894
	RMSE	0.00104	0.000184
	R^2	0.5667	0.7061
0- $1.5 Z_{eu}$	Intercept	0.00181	0.00195
	Slope	0.605	0.61
	RMSE	0.000967	0.000781
	R^2	0.7443	0.7399

114

115 Finally, our analysis indicates that the choice of the correction factor induces minor
116 changes to the b_{bp} -to-Chla relationship and little impact on the interpretation of our results. It
117 also has to be noted that regional HPLC- or radiometry-based correction factors shows some
118 limitations. The regional HPLC-based correction factors, which are potentially the most
119 robust, are for example, not available for, and therefore cannot be applied to all the regions of
120 our BGC-Argo database. BGC-Argo profiling floats sample the water column autonomously,
121 over long time periods and across different environments, likely impacting the fluorescence-
122 to-Chla relationship. HPLC-based calibration established at the time of float's deployment,
123 might be therefore less accurate over the float's lifetime. In contrast, the regional radiometry-
124 based correction factors may be applied to any BGC-Argo data provided that downwelling

125 irradiance measurements are available. However, they rely on a general empirical relationship
126 (*Morel et al.* 2007) that has been established for the surface layer only and, more critically,
127 implies that all of the world's open ocean regions show analogous bio-optical behaviour,
128 which is known not to be the case (e.g., *Organelli et al.*, 2017a). Therefore, the two sets of
129 regional HPLC- and radiometry-based correction factors proposed by *Roesler et al.* (2017)
130 provide a strong basis for examining the impact of the correction factor and of the natural
131 variability in the fluorescence-to-chlorophyll ratio on the results of our analysis. They
132 nevertheless suffer from the above limitation and thus deserve to be addressed more
133 thoroughly, especially by the collection of additional (HPLC) data set. Yet, at this stage, we
134 believe that the global correction factor is the most relevant for the present dataset.

135

136 REFERENCES

- 137 Behrenfeld, M. J., K. Worthington, R. M. Sherrell, F. P. Chavez, P. Strutton, M. McPhaden, and D. M. Shea (2006), Controls
138 on tropical Pacific Ocean productivity revealed through nutrient stress diagnostics, *Nature*, 442(7106), 1025–1028,
139 doi:10.1038/nature05083.
- 140 Blain, S. et al. (2007), Effect of natural iron fertilization on carbon sequestration in the Southern Ocean, *Nature*, 446(7139),
141 1070–1074, doi:10.1038/nature05700.
- 142 Boyd, P. W. et al. (2000), A mesoscale phytoplankton bloom in the polar Southern Ocean stimulated by iron fertilization,
143 *Nature*, 407(October), 695–702.
- 144 Cleveland, J. S., M. J. Perry, D. A. Kiefer, and M. C. Talbot (1989), Maximal quantum yield of photosynthesis in the
145 northwest Sargasso Sea., *J. Mar. Res.*, 47, 869–886.
- 146 Dubinsky, Z., and N. Stambler (2009), Photoacclimation processes in phytoplankton: Mechanisms, consequences, and
147 applications, *Aquat. Microb. Ecol.*, 56(2–3), 163–176, doi:10.3354/ame01345.
- 148 Falkowski, P., and D. A. Kiefer (1985), Chlorophyll a fluorescence in phytoplankton: relationship to photosynthesis and
149 biomass, *J. Plankton Res.*, 7(5), 715–731.
- 150 Geider, R. J., H. L. MacIntyre, and T. M. Kana (1997), Dynamic model of phytoplankton growth and acclimation: Responses

151 of the balanced growth rate and the chlorophyll a:carbon ratio to light, nutrient-limitation and temperature, *Mar. Ecol.*
152 *Prog. Ser.*, 148(1–3), 187–200, doi:10.3354/meps148187.

153 Longhurst, A. (2006), *Ecological geography of the sea*, 2nd edn. E., New York.

154 Morel, A., Y. Huot, B. Gentili, P. J. Werdell, S. B. Hooker, and B. A. Franz (2007), Examining the consistency of products
155 derived from various ocean color sensors in open ocean (Case 1) waters in the perspective of a multi-sensor approach,
156 *Remote Sens. Environ.*, 111(1), 69–88, doi:10.1016/j.rse.2007.03.012.

157 Organelli, E., F. D’Ortenzio, H. Claustre, A. Bricaud, M. Barbieux, J. Uitz, and G. Dall’Olmo (2017), Bio-optical anomalies
158 in the world’s oceans: An investigation on the diffuse attenuation coefficients for downward irradiance derived
159 from Biogeochemical Argo float measurements, *J. Geophys. Res. Ocean.*, 122, 2017–2033,
160 doi:doi:10.1002/2016JC012629.

161 Roesler, C. et al. (2017), Recommendations for obtaining unbiased chlorophyll estimates from in situ chlorophyll
162 fluorometers: A global analysis of WET Labs ECO sensors, *Limnol. Oceanogr. Methods*, 15(6), 572–585,
163 doi:10.1002/lom3.10185.

164 Schmechtig, C., H. Claustre, A. Poteau, and F. D’Ortenzio (2014), Bio-Argo quality control manual for the Chlorophyll-A
165 concentration, *Argo Data Manag.*, 1–13, doi:doi:10.13155/35385.

166 Schmechtig, C., A. Poteau, H. Claustre, F. D’Ortenzio, G. Dall’Olmo, and E. Boss (2016), Processing Bio-Argo particle
167 backscattering at the DAC level Version, *Argo Data Manag.*, 1–13, doi:doi:10.13155/39459.

168 Xing, X., A. Morel, H. Claustre, D. Antoine, F. D’Ortenzio, A. Poteau, and A. Mignot (2011), Combined processing and
169 mutual interpretation of radiometry and fluorimetry from autonomous profiling Bio-Argo floats: Chlorophyll a
170 retrieval, *J. Geophys. Res.*, 116(C6), C06020, doi:10.1029/2010JC006899.

171